Learning-based Image Analytics in User-AI Agent Interactions for Cyber-enabled Manufacturing

Mauro Lemus Alarcon*, Upasana Roy†, Anirudh Kambhampati*, Nguyen Nguyen†,
Minasadat Attari*, Ramakrishna Surya†, Filiz Bunyak*, Matthew Maschmann*,
Kannappan Palaniappan*, Prasad Calyam*
*† University of Missouri - Columbia, USA. Email: *{lemusm, akwg7, ma8pz, bunyak, maschmannm, pal, calyamp}@missouri.edu;
†{u.roy, npntz3, rst7b}@mail.missouri.edu

***Abstract*—Manual trial-and-error methods are employed for image parameter selection decisions in the processes that control cyber-enabled scientific instruments. Particularly in materials manufacturing use cases, where image analytics can be iterative, time-consuming and prone to errors, there is a need to enhance existing processes by using agents featuring learning algorithms that recommend image analytics parameters for users. In this paper, we present an analysis focused on identifying the optimal learning algorithm for an AI agent guiding real-time image processing tasks in carbon nanotube (CNT) manufacturing, which involves enhancing instrument control of cyber-enabled scanning electron microscope (SEM) instrument image scanning setup parameters such as Zoom, Focus, and Contrast. Specifically, we demonstrate the use of Reinforcement Learning (RL) and Imitation Learning (IL) based agents within a Remote Instrumentation Science Environment (RISE), a modularized system capable of utilizing multiple learning algorithms for guiding image analytics tasks. Further, we conduct a comparative performance analysis of RL and IL using 236 CNT images captured in SEM material synthesis experiments. The experiments include configuring scanning parameters for CNT images generated by SEM, implementing CNT image segmentation, and assessing the effectiveness of RL and IL agents in identifying scanning parameters to enhance image quality. The objective is to predict Zoom, Focus, and Contrast parameters using limited labeled data for offline training, guiding dynamic adjustments in SEM settings. Our findings reveal that the IL agent outperforms the RL agent under dynamic conditions in characterizing CNT image parameters - specifically, Zoom, Focus, and Contrast - by evaluating image segmentation metrics.**

***Index Terms*—user-AI agent interactions, real-time image analytics, intelligent adaptive systems, cyber-enabled manufacturing**

I. Introduction

In data-intensive scientific workflows, particularly in the materials development field, as is the case of carbon nanotube (CNT) images characterization using a scanning electron microscope (SEM) [1], researchers deal with intricate manual tasks that involve instrument calibration, data acquisition and management, and complex data analysis. Additionally, the collected datasets involve multi-dimensional parameters [2], [3], requiring specialized analytical tools for meaningful insights. Conventional manual approaches are notably laborious and result in time-consuming and error-prone processes. Image characterization plays a crucial role in the field of CNT synthesis research. Researchers rely on these results to determine, in real-time, whether the CNT growth process is progressing as expected. This enables them to take prompt actions, such as updating SEM settings, to steer the experiment in the desired direction. Implementing an automated process to assist users in analyzing CNT images promptly will enhance their decision-making abilities, ultimately improving the outcomes of the experiment.

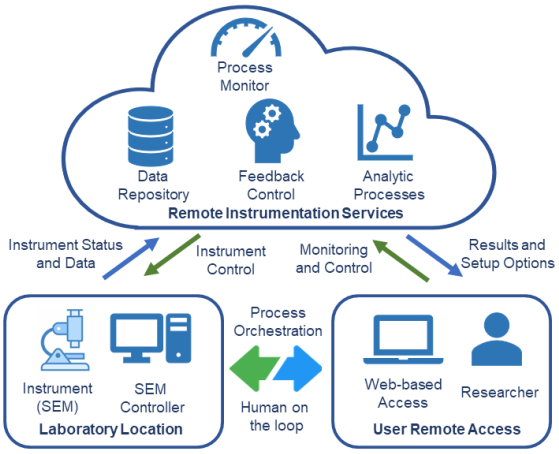

Fig. 1: Illustration of remote instrumentation with automated feedback to assist in image analytics and overcome limitations in manual processes.

To minimize the manual effort associated with the trial-and-error/time-consuming parameter selection, we can leverage remote instrumentation that employs learning algorithms within agents as illustrated in Figure 1. The implementation of closed-loop automated instrument control, as demonstrated in [4], [5], ensures the efficient and accurate operation of instruments. For novice users, the recommendations can be helpful in the selection of the most suitable SEM settings, which are critically needed e.g., in the context of growing CNTs, where minor variations in the configuration of SEM settings to capture the desired images can lead to unfavorable

This material is based upon work supported by the National Science Foundation under Award Numbers: CMMI-2026847 and OAC-2322063. Any opinions, findings, and conclusions or recommendations expressed in this publication are those of the author(s) and do not necessarily reflect the views of the National Science Foundation.

results. However, an agent-based solution requires substantial volume of images for model training [6] that are obtained from actual CNT images by altering characteristics such as Zoom, Focus, and Contrast. In addition, results from agent-based solutions may not consistently meet the desired quality, as tailoring image characteristics can induce variance in the algorithms during training [7]. Therefore, it is crucial to explore optimal learning algorithms that are effective on limited datasets for training, and can reduce the experimentation time by streamlining the entire image analytics process.

In this paper, we present an analysis focused on identifying the optimal learning algorithm for an AI agent guiding real-time image processing tasks in CNT manufacturing, which involves characterization of SEM settings in terms of Zoom, Focus, and Contrast. Specifically, we demonstrate the use of Reinforcement Learning (RL) and Imitation Learning (IL) based agents within a Remote Instrumentation Science Environment (*RISE*), a modularized system capable of utilizing multiple learning algorithms for guiding image analytics tasks. We considered RL because it showed potential in the CNT manufacturing process in prior work [8] considering CNT mechanical properties. However, given that training data can be scarce, we also considered the use of IL that is known to be suitable when working with smaller training datasets [9]. The goal of our analysis is to use the relevant RL/IL agent to predict the pertinent Zoom, Focus, and Contrast parameters in SEM settings through a chatbot interface to obtain high-quality images required for desired CNT characterization, while reducing user efforts in instrument setup. While our evaluation focused on characterizing CNT images, our methodology can be extended to address other data-intensive scientific workflow scenarios. This includes situations where image characterization can be evaluated outside of image segmentation, as seen in biomedical imaging use cases.

Through experiments, we conduct a comparative performance analysis of IL and RL under dynamic conditions using 236 CNT images captured in SEM experiments. The experiments involved configuration of preliminary scanning parameters on the SEM before capturing initial images. Subsequently, the acquired CNT images are subjected to an instance segmentation pipeline, employing the CNTSegNet [10] model — a dual loss, orientation-guided, self-supervised, deep learning network — to identify and segment CNT elements. Following segmentation, we compare the results with the RL and IL agents to evaluate which optimizes the scanning parameters to enhance image quality. Particularly, we compare the performance of the agents in predicting Zoom, Focus and Contrast parameter selections using labeled data for offline training to guide the navigation of dynamic adjustments in SEM instrument settings. To ensure result accuracy, we limit our evaluation to authentic CNT images, excluding synthetic or programmatically modified ones. Obtaining suitable CNT images through practical experimentation is challenging, and hence we rely solely on the available 256 CNT images deemed appropriate for our study.

The remainder of the paper is organized as follows: In Section II, we detail CNT characterization process workflow involving image segmentation. In Section III, we describe the learning-based SEM instrument control approach using RL/IL algorithms. In Section IV, we describe the performance comparison of the algorithms. Section V concludes the paper.

II. Image Segmentation in CNT Characterization

Herein, we introduce a CNT manufacturing use case that can benefit from remote instrumentation and real-time calibration using AI-based agents subsequent to accurate image segmentation. We specifically discuss how user-AI agent interaction can be used to predict and recommend Zoom, Contrast and Focus parameters in image acquisition tasks.

The process of growing CNT forests requires extensive preparation for in-situ experiments. Human insight is crucial to achieving desired material characteristics. High-quality images are valuable for evaluating the CNT forest structural morphology, but manual SEM scanning parameter adjustments are often time-consuming and can be error-prone due to trial-and-error. This is particularly true for novice SEM users. A dynamic setup recommendation system that optimizes SEM parameters given the latest scanned image would expedite image acquisition, reduce the need for human intervention and enhance CNT forest characterization processes significantly.

Figure 2 illustrates our Remote Instrumentation Science Environment (RISE) solution that features a closed-loop mechanism involving the CNT segmentation process using the CNTSegNet [10] deep learning pipeline. Initial scanning parameters are set by CNT manufacturing users through the SEM command controller using a web-based user interface featuring a chatbot agent. This approach employs natural language communication to provide users with the results of system inferences and interpret their actions about the changes on the SEM parameters. CNT images are processed using instance segmentation powered by ML models in CNTSegNet for CNT identification. Metrics from segmented images (i.e., Orientation Loss, Edge Coverage, Average Thickness, Average Separation, and Distance Entropy) guide RL/IL agents in predicting optimized scanning parameters (i.e., Zoom, Focus, Contrast) [11].

In addition, the chatbot agent suggests new parameters based on the characterized SEM image parameters, and upon user confirmation, the chatbot relays the parameters to the SEM command controller for instrument adjustment and execution of new image scanning. This adjustment process continues iteratively until CNT manufacturing users are content with the image quality, ensuring that subsequent experiment images are captured with the latest confirmed scanning parameters. Alternatively, users can directly interact with the SEM controller through a user interface for manual control, when immediate action is needed. By utilizing the chatbot agent's assistance, users can explore additional options for configuring SEM parameters without being constrained by a fixed set of values. They can also do so without the concern of applying values beyond reasonable limits, as the chatbot agent interacts

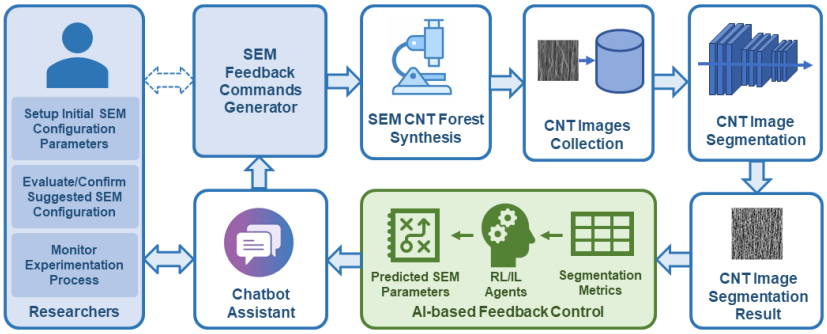

Fig. 2: Illustration of the CNT images segmentation workflow and SEM feedback control mechanism in the Remote Instrumentation Science Environment.

with users to communicate the potential outcomes of their selections.

III. Learning-based SEM Control

In this section, we detail our RL and IL based instrument control approaches, designed to tackle the issues of time-consuming and error-prone manual instrument control, especially for novice users seeking to adjust instrument settings in CNT image collection.

A. RL-based Instrument Control Approach

1) RL-based Model Description

The instrumentation control process involves optimizing a decision-making process with five input parameters (Orientation Loss, Edge Coverage, Average Thickness, Average Separation, and Distance Entropy) used to determine three distinct setup action values (Zoom, Focus, Contrast). The objective is to determine the best action values, aiming to achieve the best possible settings for an SEM on obtaining ideal CNT images. This decision-making task poses a challenge due to the complex multi-input and multi-output nature of the CNT manufacturing problem.

Given the heuristic nature of providing dynamic-parameter recommendations, and the need to uncover optimal strategies in a complex parameters action space, we selected Q-Learning [12], [13], a reinforcement learning technique which is suitable as a potential solution to address these complexities and discover optimal action-selection strategies. The key component of this technique is the Q-value function, also referred to as the action-value function, which represents the state-action relation. The Q-value function is derived from the the Bellman equation, a recursive mathematical expression used in RL to represent the expected cumulative reward (Q-value) assigned to an agent for taking a specific action in the current state of the environment [14]. The Q-value function $Q(s, a)$ takes two inputs parameters the current state and an action, and predicts a new state, which is intended to increase a cumulative reward that an agent would earn by acting in state s and then adhering to the best course of action a. Below we elaborate on the description of the state space, action space, and Q-value function in the context of our CNT images scanning and image optimization.

State space: The state space defines all potential combinations of values of the five CNT images segmentation metrics. This five-dimensional space defines a current (AT, AS, EC, OL, DE) and predicted next (ATt, ASt, ECt, OLt, DEt) state of our SEM setup. Where, AT: Average Thickness; AS: Average Separation; EC: Edge Coverage; OL: Orientation Loss; DE: Distance Entropy. From a current state, the agent proceeds to the next state by choosing the best action calculated by the Q-Learning Equation 1.

$$Q(s,a)^* \leftarrow Q(s,a) + \alpha[r + \gamma max(Q(s^1, a^1)) - Q(s,a)] \tag{1}$$

Where, $Q(s,a)^*$ is the Q-value, representing the expected cumulative reward for taking action a in state s; r is the immediate reward obtained by taking action a in state s; α is the learning rate determining the impact of new information on the Q-value; γ is the discount factor balancing immediate and future rewards; $\max(Q(s', a'))$ represents the maximum Q-value achievable in the next state s'; s' is the subsequent state; and, a' is the optimal action in the next state. In the context of the CNT image characterization, state s represents the current value of the CNT image segmentation results (AT, AS, EC, OL, DE); action a represents the agent's decision of selecting specific zoom, focus, and contrast values for the given CNT image; and, the reward r is given by the accuracy of the agent in inferring the right CNT zoom, focus, and contrast values of the CNT image being evaluated.

Action space: The action space includes all possible options for the setting parameters (Zoom, Focus, Contrast) that can be selected to setup the SEM instrument. Given a current state s and action a, the probability of each possible pair of next state ($s1$) and reward (r), is defined by Equation 2.

$$p(s^1, r|s, a) = P_r\{S_{t+1} = s^1, R_{t+1} = r|S_t = s, A_t = a\} \tag{2}$$

2) RL-based Instrument Control

Algorithm 1 implements our Q-learning, an RL-based approach for CNT image scanning optimization for real-time calibration. This algorithm is used to train our RL agent on learning an optimal policy to predict the Zoom, Focus and Contrast. In this case, the environment represents the image segmentation metrics where the agent (the Q-learning algorithm) takes prediction actions that are suitable to optimize the quality of the CNT image. The segmentation parameters

Algorithm 1: Update State and Calculate Reward

Require: action: Chosen action, previous rewards for Zoom, Focus, and Contrast
Ensure: reward: Calculated reward, flag: Flag indicating state update, state_data: Dictionary of Zoom, contrast, and focus

reward ← 0
alpha ← 0.001
discount_factor ← 0.999
Zoom ← state['AT'] × state['AS']
focus ← state['EC']
contrast ← state['OL'] × state['DE']
prev_q_value ← 0 {Initialize prev_q_value}
UPDATE_STATEstate, alpha, gamma, reward, prev_action, q_values {Update Zoom, focus, and contrast based on Q-Learning formula}
prev_q_value ← q_values[prev_action]
max_q_value_next_state ← max(q_values)
td_error ← reward + discount_factor × max_q_value_next_state - prev_q_value
q_values[prev_action] ← prev_q_value + alpha × td_error
state['AT'] ← Zoom × state['AT']
state['AS'] ← Zoom × state['AS']
state['EC'] ← focus × state['EC']
state['OL'] ← contrast × state['OL']
state['DE'] ← contrast × state['DE']
flag ← False
state_history.append(state)
action_history.append(action)
return state, reward, flag, {'Zoom': [Zoom], 'contrast': [contrast], 'focus': [focus]} =0

(i.e., Orientation Loss, Edge Coverage, Average Thickness, Average Separation and Distance Entropy) are used as features to evaluate the quality of the image. They provide information about the performance of the image processing algorithm based on the chosen parameters. The environment provides feedback in the form of rewards based on the agent's action taken in each state. The algorithm iteratively explores the environment, refines its actions, and converges to an optimal solution over time. Our RL agent code is available here [15].

B. IL-based Instrument Feedback Control Approach

1) IL-based Model Description

IL, also known as behavioral cloning or learning from demonstrations [16], is a type of machine learning technique used in the field of artificial intelligence. It involves learning a behavior by imitating the actions of a demonstrator. In this approach, an agent observes the expert's behavior as demonstrations and tries to learn a mapping between the observed states and the corresponding actions taken by the expert. Traditionally, supervised learning requires vast amounts of labeled data to achieve accurate results, however, IL has been proven to perform well under limited availability of training data. In domains where generating this labeled data is a challenge, IL emerges as an suitable solution. By imitating expert demonstrations, our model learns to make predictions for unseen situations. Our specific problem revolves around predicting three distinct but interrelated actions – Zoom, Focus, and Contrast – based on five input features Orientation Loss, Edge Coverage, Average Thickness, Average Separation, and Distance Entropy related to image quality and composition. This problem can be addressed by training the IL agent using actual CNT image segmentation metrics and its Zoom, Focus, and Contrast characteristics, so the agent learns how to adjust these parameters based on the given image segmentation metrics aiming to predict similar parameters of the images used in the training process.

Gradient Boosting Regressor: In our IL-based feedback command agent approach, we employ a Gradient Boosting Regressor [9] architecture individually for predicting each target label. It aims to produce a prediction model in the form of an ensemble of weak prediction models, typically decision trees. The idea is to add new models to correct the errors made by existing models. Models are added sequentially until no further improvements can be made. Mathematically [17], the prediction of the ensemble model F is described by Equation 3.

$$F(x) = \sum_{m=1}^{M} \gamma_m h_m(x) \tag{3}$$

Where M is the number of trees, $h_m(x)$ is the m-th tree, and γ_m is the learning rate. A smaller learning rate means each tree will correct fewer errors of its predecessors, requiring more trees but often resulting in a more robust model. Subsampling controls the fraction of samples used for fitting the individual base learners. It introduces randomness into the ensemble, aiding in making the model robust against overfitting, and is a form of Stochastic Gradient Boosting. The model's performance (see **Algorithm 2**) is evaluated using 5-fold cross-validation, as indicated by *KFold* (n_splits=5). In other words, our dataset (see Section IV-A) is divided into 5 parts, and in each iteration, 4 parts are used for training while 1 part is used for validation. In this context, the learning algorithm is trained and evaluated five times, each time using a different fold as the validation set and the remaining folds as the training set. The process is repeated 5 times, ensuring each fold serves as a validation set once. The data is shuffled ($shuffle$ = True) before splitting, and the setting of $random\_state$ = 42 ensures reproducibility of the splits. The purpose of using 5-fold cross-validation is to obtain a more robust estimate of the model's performance by reducing the impact of the specific subset used for validation. This also helps to ensure that the model's performance is representative across different portions of the dataset.

Hyperparameter Tuning: The hyperparameters of the Gradient Boosting Regressor (see **Algorithm 2**) are optimized using a grid search. This means that the model will be trained and validated on every possible combination of the provided hyperparameters in *param_grid*. These hyperparameters are chosen to achieve a balance between making the model complex enough to capture underlying patterns and relationships in the data (low bias), but not so complex that it fits to noise and peculiarities of the training data (high variance). Once the grid search completes, the best hyperparameters are extracted with *grid_search.best_params*, and the best model (with the optimal hyperparameters) is extracted with *grid_search.best_estimator*. We use Root Mean Squared Error (RMSE) as the scoring metric in the grid search as defined by Equation 4.

$$RMSE = \sqrt{\frac{\sum_{i=1}^{n}(Y_{\text{true},i} - Y_{\text{pred},i})^2}{n}} \tag{4}$$

Where $Y_{\text{true},i}$ are the true values, $Y_{\text{pred},i}$ are the predicted values, and n is the number of samples.

In our imitation learning approach, RMSE is most suited for CNT image characterization due to its focus on error magnitude, which is crucial for accurately estimating features such as zoom, focus, and contrast. The error magnitude is also essential because it provides significance to larger errors, ensuring that substantial deviations in predicting features are appropriately considered in evaluating the model's performance. In contrast, metrics such as mean absolute error (MAE), R-squared, mean squared error (MSE), and Percentage of Variance Explained may not adequately capture the importance of error magnitudes or align with the specific requirements of CNT image parameter prediction. For example, MAE treats all errors equally, R-squared prioritizes explaining variance over error magnitudes, MSLE is designed for proportional predictions, and Percentage of Variance Explained may be more suitable for elucidating variability rather than the accuracy of specific predictions.

2) IL-based Instrument Control

The **Algorithm 2** outlines the process of training an agent (Gradient Boosting Regressor model) using a given set of input features (the independent variables) and predicting multiple target variables (the dependent variables) from given input features. Since IL is a form of Supervised Learning [18], it is trained as in the case of any Supervised Learning algorithm. The algorithm displayed is for predicting any one target variable at a time, for example Zoom, but the same algorithm with different hyperparameters as mentioned in Table II can be used to predict Focus and/or Contrast.

Algorithm 2: Gradient Boosting Regression

Input: Orientation_Loss, Edge_Coverage, Average_Thickness, Average_Separation, Distance_Entropy
Output: Zoom

$X \leftarrow Input$
$Y \leftarrow Output$
$model \leftarrow$ **GradientBoostingRegressor**$(random\_state = 0)$
$wrapper \leftarrow$ **MultiOutputRegressor**$(model)$
$kfold \leftarrow$ **KFold**$(n\_splits = 5, shuffle = True, random\_state = 42)$
$param\_grid \leftarrow \{...\}$
$grid\_search \leftarrow$ **GridSearchCV**$(wrapper, param\_grid, cv = kfold, ...)$
$grid\_search.$**fit**(X, Y)
$best\_params \leftarrow grid\_search.best\_params\_$
$best\_model \leftarrow grid\_search.best\_estimator\_$
$Y\_pred \leftarrow best\_model.$**predict**$(X\_test)$
$mse \leftarrow$ mean_squared_error$(Y_test, Y_pred, multioutput = 'raw_values')$
rmse $\leftarrow$ **np.sqrt**(mse)

The algorithm begins by loading and preprocessing the input data, including features such as Orientation Loss, Edge Coverage, Average Thickness, Average Separation, and Distance Entropy. The data is then split into training and testing sets. The input features and target variables are normalized to ensure stable convergence during training. A Gradient Boosting Regressor model is constructed and compiled, followed by training using the normalized training data. The model is evaluated on the test set, and the RMSE values are used as the evaluation metric. Predictions are made on the test set using the trained model, and the predicted probabilities are inverse-transformed to their original scale using a scaler. The final step involves returning the predicted values for Zoom, Focus, and Contrast. Our IL agent code is available here [19].

IV. Performance Evaluation

In this section, we first describe our SEM CNT images data set. Following this, we discuss the performance comparison of the RL/IL agent based instrument control approaches in selection of the SEM parameters for guiding the CNT image analytics process.

A. SEM CNT Images Data Set

To conduct offline training for our RL and IL agents, we gathered actual CNT images from the SEM, ensuring they met the required quality standards. This dataset comprises of images with three different Zoom magnification levels (25000, 50000, 100000), Focus values ranging from 5.8 to 8.9, and Contrast values ranging from 58.5 to 72.9. Out of the total 236 data images, 80% are allocated for training the model, while the remaining 20% are reserved for testing. The test dataset comprises 48 samples, with 20 from a Zoom of 25000, 20 from a Zoom of 50000, and 8 from a Zoom of 100000. This intentional uneven distribution ensures an optimal training-to-testing data ratio for each Zoom category. Through CNT segmentation, we derived five evaluation metrics (Orientation Loss, Edge Coverage, Average Thickness, Average Separation, and Distance Entropy). Utilizing these segmentation metrics results, we trained our RL and IL agents to predict three SEM setup parameters (Zoom, Focus, Contrast) with the aim of scanning CNT images comparable in quality to the original ones. The CNT dataset is publicly accessible at [19].

B. RL-based feedback control experiments results

Utilizing our CNT dataset, we have deployed a tailored image environment designed for our RL tasks. This environment features a multi-dimensional state space (see **Algorithm 1)**, capturing key image quality metrics such as Orientation Loss, Edge Coverage, Average Thickness, Average Separation, and Distance Entropy. These metrics emulate the settings of a SEM, with actions corresponding to adjustments in Zoom, Focus, and Contrast levels. To ensure meaningful training, we have established a reward structure that incentivizes SEM settings leading to target image quality, defined by specific thresholds for each metric. Simultaneously, actions outside the permissible range incur penalties. Throughout training, the environment tracks both state and action histories, facilitating subsequent analysis.

Through RL, our agent iteratively refines SEM settings to attain the desired image quality. In training, the RL agent explores the state space, takes actions, observes rewards, leveraging this experience to enhance its policy. In our RL-based architecture, hyperparameters, as outlined in Table I, produce results shown in Figure 3. However, Q-learning faces challenges in scenarios with complex exploration-exploitation dynamics, struggling in our environment with five states and

Hyperparameter	Value
Learning Rate	0.001
Discount Factor	0.999
Exploration Probability	0.1
Number of episodes	1000

TABLE I: Hyperparameters used in **Algorithm 1** to tune and recommend suitable parameters.

three actions, leading to slow convergence and suboptimal policies despite tuning the hyperparameters along with the reward. Additionally, the Q-learning sensitivity to hyperparameter choices further influences its performance in our experiments.

C. IL-based feedback control experiments results

We have implemented a Gradient Boosting Regressor which is an ensemble machine learning technique that constructs a model by optimizing the addition of individual models, in this case, decision trees. This model is wrapped inside a *MultiOutputRegressor* (see **Algorithm 2**), although, in this instance, only one target at a time is being predicted. A 5-fold cross-validation strategy is set up using *KFold* with shuffling enabled. A Grid Search is set up using the *GridSearchCV* method. Grid search is used to perform hyperparameter tuning to determine the optimal values for a given model. The scoring metric used during the grid search is the negative mean squared error, which means the model aims to minimize the mean squared error during training.

Hyperparameters	Zoom	Focus	Contrast
N Estimators	100, 200, 300	50, 100, 150, 200	50, 100, 150, 200
Learning Rate	0.001, 0.01, 0.05	0.01, 0.05, 0.1	0.001, 0.01, 0.05, 0.1, 0.5
Max Depth	2, 3, 4	3, 4, 5	3, 4, 5
Min Samples Split	3, 4, 5	2, 4	2, 4, 6, 8
Min Samples Leaf	2, 3	1, 2	1, 2
Subsample	0.7, 0.8, 0.9	0.8, 1.0	0.5, 0.7, 0.8, 0.9, 1.0
Max Features	'sqrt', 'log2', None	'sqrt', 'log2', None	'sqrt', 'log2', None

TABLE II: Hyperparameter grid set used in **Algorithm 2** to tune and recommend suitable parameters.

The IL model was moderately able to learn the different variations and intricacies around our current data points. For Zoom, the number of hyperparameter combinations tested are 1458, total fits performed are 7290 and the RMSE of Zoom is 0.23187. For Focus, the number of hyperparameter combinations tested are 864, total fits performed are 4320 and the RMSE of Focus is 0.42572. For Contrast, the number of hyperparameter combinations tested are 36000, total fits performed are 180000 and the RMSE of Contrast is 0.77316. The RMSE for Zoom is the best (lowest), suggesting good model performance for predicting Zoom, followed by Focus, followed by Contrast which has the worst (highest) RMSE, indicating poorer predictive performance in the Contrast data as CNTSegNet model [10] performs auto correction of contrast or internal contrast normalization. Figure 4 shows our key finding of how the predicted outcomes when subjected to validation against actual results reveal that IL-based model predictions outperform the RL-based model consistently. We remark that the Zoom prediction faced challenges in the RL-based model, however the IL-based model in the same case was effective.

D. Challenges on training the RL and IL models

We obtained meaningful results using our RL and IL approaches for determining the zoom, focus and contrast parameters by analyzing the segmentation metric of CNT images. However, these approaches pose challenges in applying them for our purpose. For instance, while validating our predicted results against the actual results, it was observed that the IL predictions gave better results compared to the RL predictions. The prediction of Zoom was not effective using the RL-based model, however it was handled effectively by the IL-based model. However, the IL-based model could not perform well with predicting Contrast, which is a limitation. Further, we found that the IL-based model encountered was not effective in adeptly predicting Contrast, revealing another limitation in our approach. The RL-based model was highly ineffective with the prediction of Zoom which was handled very effectively by the IL-based model. Some of these results' flaws can be attributed to the fact that we have a limited set of images for training, which is a factor we need to handle due to the Contrast setup in getting more real CNT images.

V. Conclusion

In this paper, we compared RL and IL agent based approaches to identify the optimal learning algorithm to guide real-time image processing tasks in CNT manufacturing on cyber-enabled SEM instruments. The RL-based approach used a Q-Learning based algorithm to generate recommendations for an SEM to capture quality images while scanning. In addition, the IL-based approach used a functional-gradient approach to imitate an expert in action to recommendations image scanning parameters for a SEM setup. These algorithms were integrated into a RISE solution that allows the learning algorithms and a chatbot-based service to enable user-AI agent interactions. Thus, RISE allowed users to directly interface with cyber-enabled instruments using a suite of RL and IL agents that can be integrated as plug-ins for instrument control, and transform time-consuming and error-prone manual CNT manufacturing processes. Our results emphasize the success of IL over RL in enhancing Zoom, Focus, and Contrast predictions, with quicker convergence and reduced sample requirements.

Future work could involve providing iterative feedback control to predict and recommend parameters for improving the quality of CNT images, based the characterization of parameters of ideal CNT images. In addition, future work could involve expanding the RISE system with web services that integrate our RL/IL algorithms for a broader range of image analytics applications.

References

[1] Ryan Hines, Taher Hajilounezhad, Cole Love-Baker, Gordon Koerner, and Matthew R Maschmann. Growth and mechanics of heterogeneous, 3d carbon nanotube forest microstructures formed by sequen-

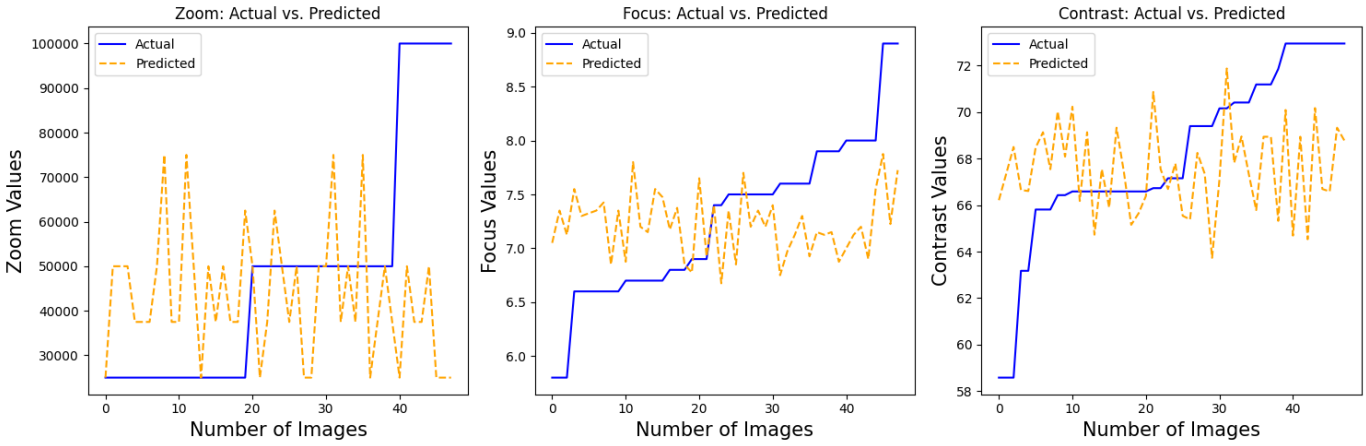

Fig. 3: RL-based Actual vs. Predicted Zoom, Focus and Contrast after hyperparameter tuning from Table I.

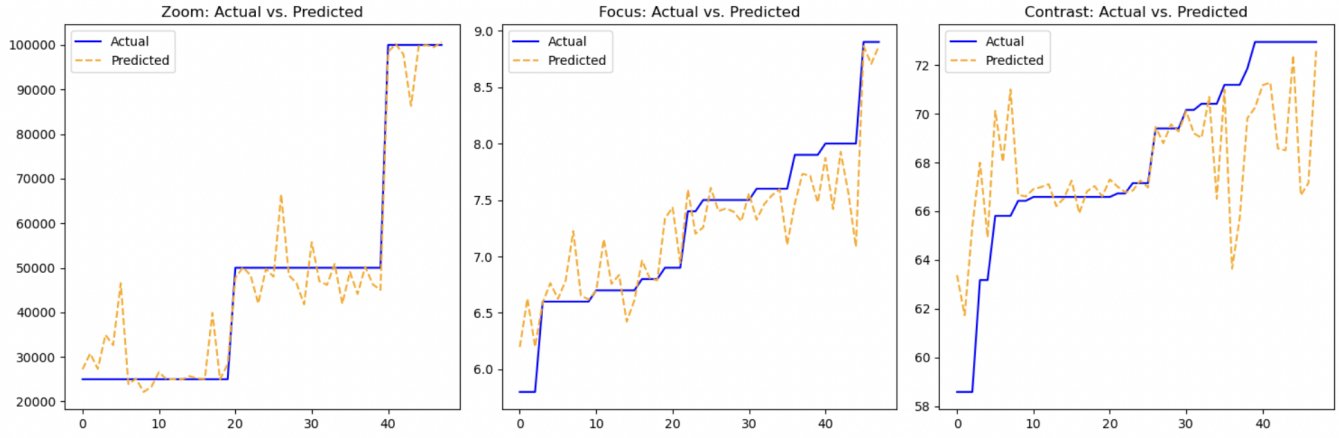

Fig. 4: IL-based Actual vs. Predicted Zoom, Focus and Contrast after hyperparameter tuning from Table II.

tial selective-area synthesis. *ACS applied materials & interfaces*, 12(15):17893–17900, 2020.

[2] Taher Hajilounezhad, Damola M Ajiboye, and Matthew R Maschmann. Evaluating the forces generated during carbon nanotube forest growth and self-assembly. *Materialia*, 7:100371, 2019.

[3] Taher Hajilounezhad, Rina Bao, Kannappan Palaniappan, Filiz Bunyak, Prasad Calyam, and Matthew R Maschmann. Predicting carbon nanotube forest attributes and mechanical properties using simulated images and deep learning. *npj Computational Materials*, 7(1):134, 2021.

[4] Jorge Mireles, Cesar Terrazas, Sara M Gaytan, David A Roberson, and Ryan B Wicker. Closed-loop automatic feedback control in electron beam melting. *The International Journal of Advanced Manufacturing Technology*, 78:1193–1199, 2015.

[5] Takayuki Osa, Christoph Staub, and Alois Knoll. Framework of automatic robot surgery system using visual servoing. In *2010 IEEE/RSJ International Conference on Intelligent Robots and Systems*, pages 1837–1842, 2010.

[6] Dharmesh Tailor and Dario Izzo. Learning the optimal state-feedback via supervised imitation learning. *Astrodynamics*, 3:361–374, 2019.

[7] https://www.mccrone.com/mm/3-tips-improving-sem-image-quality/.

[8] Ashish Pandey, Ramakrishna Surya, Matthew Maschmann, and Prasad Calyam. Reinforcement learning based carbon nanotube growth automation. In *2021 IEEE Applied Imagery Pattern Recognition Workshop (AIPR)*, pages 1–10. IEEE, 2021.

[9] Sriraam Natarajan, Saket Joshi, Prasad Tadepalli, Kristian Kersting, and Jude Shavlik. Imitation learning in relational domains: A functional-gradient boosting approach. In *IJCAI proceedings-International joint conference on artificial intelligence*, volume 22, page 1414, 2011.

[10] Nguyen P Nguyen, Ramakrishna Surya, Matthew Maschmann, Prasad Calyam, Kannappan Palaniappan, and Filiz Bunyak. Self-supervised orientation-guided deep network for segmentation of carbon nanotubes in sem imagery. In *Computer Vision–ECCV 2022 Workshops: Tel Aviv, Israel, October 23–27, 2022, Proceedings, Part VIII*, pages 412–428. Springer, 2023.

[11] Scanning electron microscopy. https://www.nanoscience.com/techniques/scanning-electron-microscopy/. Accessed: Jan 12, 2024.

[12] Jesse Clifton and Eric Laber. Q-learning: Theory and applications. *Annual Review of Statistics and Its Application*, 7:279–301, 2020.

[13] Martijn Van Otterlo and Marco Wiering. Reinforcement learning and markov decision processes. In *Reinforcement learning: State-of-the-art*, pages 3–42. Springer, 2012.

[14] Zihan Ding, Yanhua Huang, Hang Yuan, and Hao Dong. Introduction to reinforcement learning. *Deep reinforcement learning: fundamentals, research and applications*, pages 47–123, 2020.

[15] Anirudh Kambhampati. Rlcode: Rl code to provide parameter feedback, 2023. Dataset, 2023. Accessed: October 26, 2023. Available at http://bit.ly/3SHx0yU.

[16] Faraz Torabi, Garrett Warnell, and Peter Stone. Behavioral cloning from observation. *arXiv preprint arXiv:1805.01954*, 2018.

[17] Yanru Zhang and Ali Haghani. A gradient boosting method to improve travel time prediction. *Transportation Research Part C: Emerging Technologies*, 58:308–324, 2015.

[18] James MacGlashan and Michael L Littman. Between imitation and intention learning. In *Twenty-fourth international joint conference on artificial intelligence*, 2015.

[19] Imitation Learning Code and Dataset, 2023. Accessed: October 26, 2023. Available at https://bit.ly/ImitationLearningCodeAndDataset.